

# MINERAL GRAIN SPATIAL PATTERNS AND REACTION RATE UP-SCALING

C. A. PETERS<sup>1</sup>, J. A. LEWANDOWSKI, M. L. MAIER, M. A. CELIA AND L. LI

<sup>1</sup> *Department of Civil & Environmental Engineering, Princeton University, Princeton, NJ 08544, U.S.A. cap@princeton.edu*

## ABSTRACT

Reactive transport models that describe mineral reactions in porous media rely on laboratory measurements of rate parameters that may fail to represent reactions defined at larger averaging scales. In recently completed work, we used pore-scale network models to investigate the effects of heterogeneities in pore structure and mineral distribution on geochemical reaction rates in porous media. Our findings revealed significant scaling effects from variations in reactive mineral distribution, especially for the highly acidic conditions encountered in geological sequestration of carbon dioxide. In this paper we present preliminary findings from electron scanning BSE maps, to analyze spatial patterns of minerals in sedimentary rocks. Samples include sandstones from the Viking formation in the Alberta basin in western Canada. Image analysis was used to quantify pore space and examine reactive minerals in relation to pore locations. Typically, reactive minerals occur as distinct grains and inclusions, and their percent abundance is larger than the extent of their contact with pore fluids.

## 1. INTRODUCTION

Accuracy in reactive transport modeling is compromised if reaction rate parameters are based on measurements at a spatial scale that is not relevant to the spatial resolution of the model. Kinetics for geochemical reactions that describe mineral dissolution and precipitation are typically measured in the laboratory using crushed minerals in well-mixed systems (e.g. White and Brantley, 1995). These rates accurately describe so-called surface-controlled reaction kinetics but they are of questionable value in porous media in which mass transport often plays a governing role.

In this work, we address the problem of up-scaling geochemical reaction rates from the scale of individual pores (10 to 100  $\mu\text{m}$ ) to the scale of a network of pores in a porous medium (mm to cm). At the porous medium scale, reaction rates are affected by the pore network heterogeneities that affect fluid flow and by the spatial distributions of reactive minerals throughout the pore network.

Several decades of research have focused on the impacts of physical heterogeneities on permeability (e.g. Dagan 1990; Wallstrom et al. 1999; Christie and Blunt 2001), and the resulting mathematical representation of mechanical dispersion (e.g. Glimm et al. 1993; Neuman and Orr 1993). With a few notable exceptions related to sorption reactions (Espinoza and Valocchi, 1997; Tompson, 1993), surprisingly little attention has been paid to chemical heterogeneities and the scale effects for geochemical reactions. Understanding these scale effects is critically important to applications of reactive transport modeling involving

geochemical reactions (Steeffel and Lasaga 1994, Lichtner et al. 1996, Bryant and Thompson 2001). An example is the application of reactive transport modeling to geological sequestration of CO<sub>2</sub> in which highly acidic conditions cause silicate and carbonate dissolution, and precipitation of clays and new carbonates (Xu et al. 2003, Knauss et al. 2005, Bruant et al. 2002).

At Princeton, and with collaboration from Dr. Lindquist at SUNY Stony Brook, we are using a combination of electron scanning techniques and computational simulation to investigate heterogeneities in pore structure and mineral distribution and the effects on geochemical reaction rates in porous media. In this paper, we focus on the spatial patterns of mineral grains in sedimentary rock thin sections, analyzed using scanning electron microscopy in backscatter mode. This paper also presents an overview of recently completed computational work in which we developed pore-scale network models to explore scaling effects. The electron scan findings are discussed in the context of the modeling results.

## 2. MATERIALS AND METHODS

### 2.1 Sedimentary Rock Samples

The sedimentary rock samples used in this work are sandstones from the Alberta sedimentary basin in western Canada. The sedimentary succession in this basin, and associated lithology and hydrostratigraphy, are described by Bachu, et al. (1994). Core samples come from the Viking formation, taken at depths ranging from 2000 to 4000 m. Viking sandstones are calcareous litharenites, with porosities (mostly primary) ranging from 1% to 24% and permeabilities ranging from 0.01 to 1000 md (Kreutzer-Walz, 2005). The cores are from oil and gas wells, active and abandoned, from a wide area of the formation within a 320 km radius of Edmonton. In addition to the mineralogical imaging of these samples being done at Princeton, Dr. Lindquist is using synchrotron X-ray computed microtomography imaging together with 3DMA-Rock to analyze pore structures and surface areas (e.g. see Jones et al. 2003).

### 2.2 Specimen Preparation and Backscatter Electron Mapping

The samples, 11-27-023-03w4, 10-19-056-10w4, and 06-32-059-14w5, were cut collinear to the axes of the sample cores and may be qualitatively described as sandstone, shaly sandstone, and conglomerate sandstone, respectively. Specimen preparation, done by FPC Geological Labs, included thin sectioning, impregnating with epoxy resin, adhering to rectangular glass slides, and polishing. At Princeton, the VCR IBS/TM250 Ion Beam Sputterer was used to add 25 nm of conductive carbon coating to each slide, to prevent charge buildup on the sample surface.

Backscatter electron (BSE) mapping was used to produce gray scale images of sedimentary rock samples on the basis of compositional contrast. Images were produced on the FEI XL30 FEG-SEM at Princeton's Imaging and Analysis Center, using a beam intensity of 20 kV and a working distance of 15 mm. Backscattering occurs when high-energy electrons are deflected by atomic nuclei at angles greater than 90° and ejected from the sample (Reed, 1996). Since the amount of electron backscatter is proportional to atomic number in pure elements and mean atomic number in compounds, BSE maps provide useful information regarding the mineralogy of geological samples. Images were produced at a beam

resolution of 2nm, with pixel resolutions on the order of 1  $\mu\text{m}$ . The BSE images presented here were taken at a magnification of 100x.

### 2.3 Image Processing

BSE images were analyzed using the Image Processing toolbox in MATLAB (Mathworks Release 14). The images were processed with the objective of mapping pore space, quartz, and other minerals, and quantifying the relative areas associated with these classes. In a BSE image, pore space is evident as black, i.e. the absence of backscattered electrons. For each image, the pixel range for quartz was identified by visual inspection of the intensity histogram combined with detailed pixel imaging of selecting quartz grains. The two remaining pixel ranges were those that have lighter intensities than pore space but darker than quartz and those that have lighter intensities than quartz. Color images were produced using the color scheme indicated in Table 1. Black and white images were also produced to show only pore space. Using pixel counts, the fractional areas for each of the four classes were computed.

TABLE 1. Color mapping scheme used to process BSE images.  
Source for mean atomic numbers, in this table and throughout: Krinsley et al. 1998.

Mean Atomic Number	Color Map
<i>None</i> (Pore Space)	Black
Smaller than quartz	Green
10.80 (Quartz)	Grey
Larger than quartz	Red

## 3. IMAGING RESULTS

Figure 1 shows two images of the same conglomerate sandstone. The SEM image reveals mostly topographic irregularities arising from uneven specimen coating, thus obscuring important geological information. The BSE image reveals the chemical uniformity of the mineral and clearly indicates pore space. The sensitivity of BSE mapping to compositional contrasts reveals mineral inclusions (white spots) in the grains, which are impossible to detect in SEM imaging. This comparison illustrates the value of BSE mapping for study of geological samples.

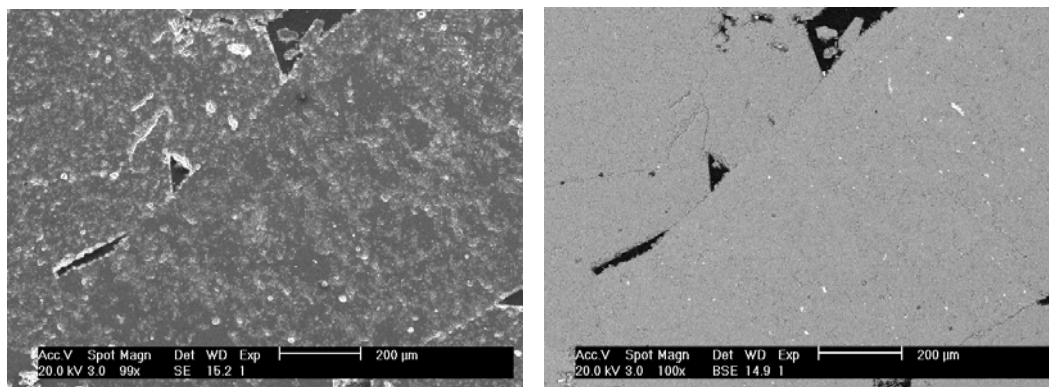


FIGURE 1. SEM (left) and BSE (right) image of a conglomerate sandstone 06-32-059-14w5.

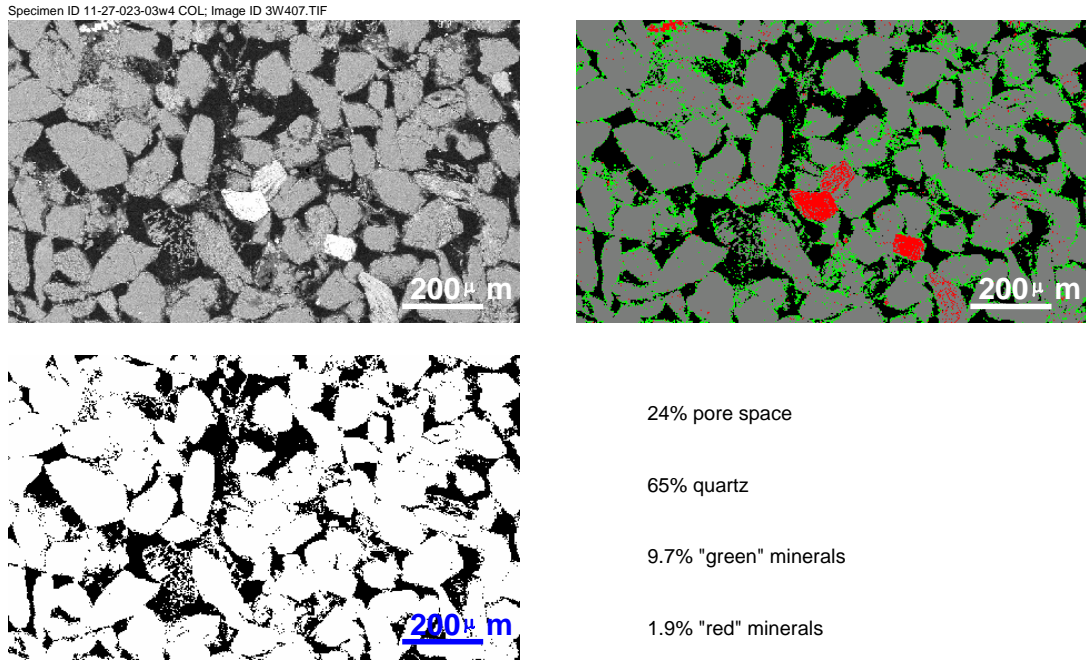


FIGURE 2. Sandstone 11-27-023-03w4 100x. *Upper left*: BSE greyscale image. *Upper right*: Color-processed BSE image. *Lower left*: Processed BSE image showing only pore space.

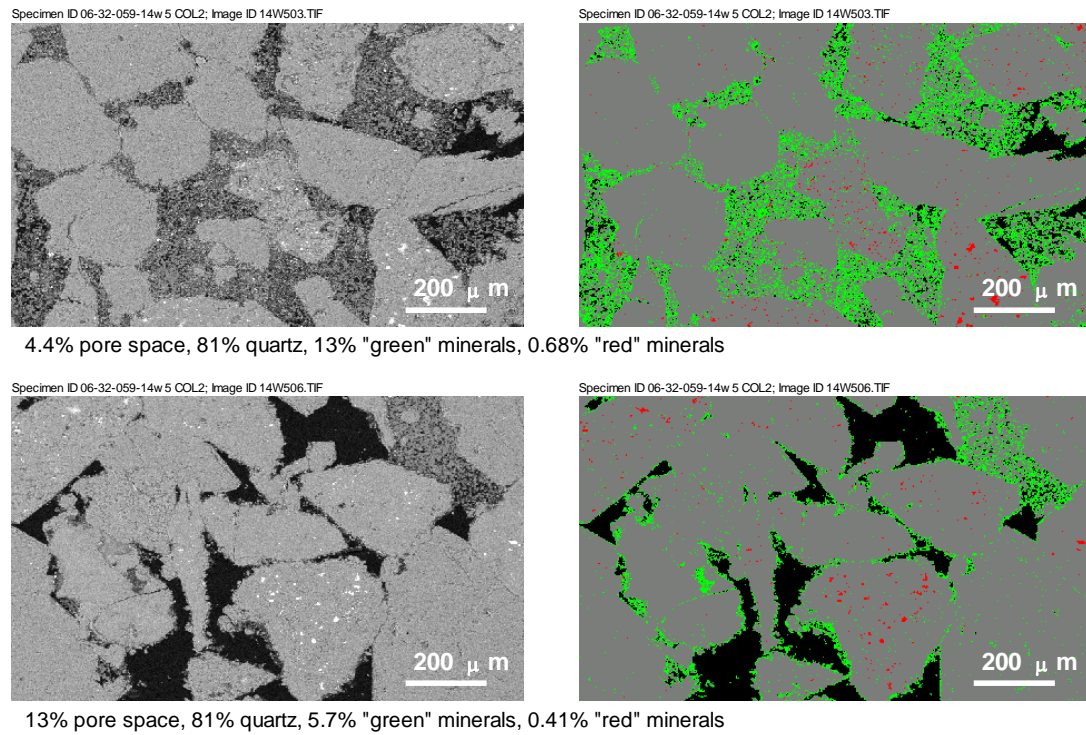


FIGURE 3. Conglomerate sandstone 06-32-059-14w5 COL2 100x. BSE greyscale (*left*) and color-processed images (*right*) for two spots on the same thin section.

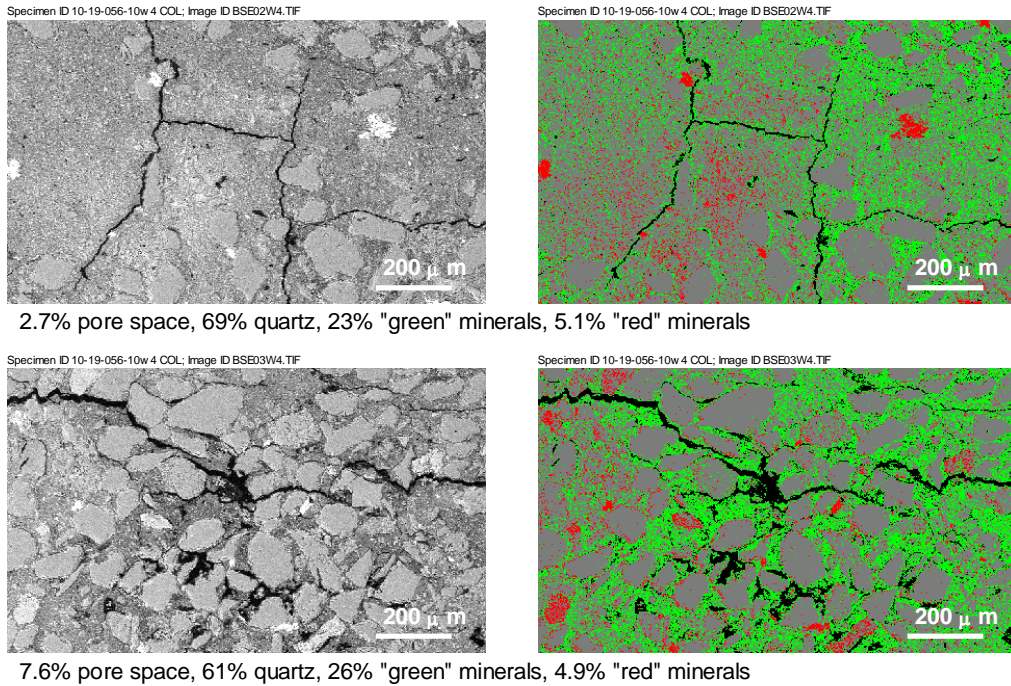


FIGURE 4. Shaly sandstone 10-19-056-10w4 COL 100x. BSE greyscale (*left*) and color-processed (*right*) images for two spots on the same thin section.

Figure 2 shows different forms of a BSE image of sandstone. The BSE image provides valuable information about grain size, shape and sorting. The greyscale BSE map provides some information about mineral differences, particularly for minerals with large mean atomic number which appear white. It is much more difficult to use the greyscale map to distinguish quartz grains from the cements between grains because of the similarity in intensities of grey color.

The color-processed BSE image visually enhances these distinctions. In this sandstone the “green” mineral (which is probably just one mineral species) is an authigenic precipitate that cements quartz grains. It is possibly kaolinite, which has a mean atomic number of 10.24 and is one of only a few minerals with mean atomic number smaller than quartz. The minerals in the “red” category, which account for only 1.9% of the total area, are seen as inclusions in quartz grains or as distinct grains. Identification of the chemical formulas of these minerals will require energy dispersive X-ray spectroscopy.

BSE imaging provides a useful means of evaluating the size, shape and total volume of pores in consolidated rocks. The pore space image in Figure 2 reveals primary pores as large as 100  $\mu\text{m}$ , as well as micropores within matrix minerals. The spatial resolution of the images presented in Figure 2 allows inspection of pores on the length scale of 1  $\mu\text{m}$ . Based on an area analysis of this small sample, the porosity is 24%.

Figure 3 shows two sets of images for the same thin section of a conglomerate sandstone. Both have the same densities of quartz grains, but they have remarkably different quantities of authigenic precipitates. The difference in pore space is entirely related to the difference in cement (green) between quartz grains, which indicates that primary pore space was originally equal but local weathering and precipitation was very different.

A Viking shaly sandstone (Figure 4, two views) has substantially less pore space than the non-shaly sandstones, and the pore space is in the form of fractures rather than interstitial space. The amount of quartz in the shaly sandstone is not substantially different from the amounts in the non-shaly sandstones in Figures 2 and 3, but the quartz grains in the shaly sandstone is highly cemented. The shaly sandstone is also substantially different from the other sandstones in the relative amount of non-quartz minerals, account for approximately 30% of the total volume.

#### 4. NETWORK MODELING OF REACTION RATE UP-SCALING

Pore-scale network models provide a mathematical tool that combines pore-level descriptions of fluid flow over many interconnected pore elements to produce a description at the scale of a porous medium continuum. Development of network models to simulate geochemical reaction kinetics is a novel application of such models, which previously have focused on two-phase flow in porous media, interphase mass transfer and biofilm growth. Our recent network modeling work (Li et al 2004, 2006) involves reactive flow and transport simulations in physically and chemically heterogeneous networks of pores. Reactive transport processes are simulated at the pore scale, and mass balance principles are used to calculate reaction rates at the scale of the entire network. To examine the scaling behavior of reaction kinetics, these rates are compared to rates calculated by assuming spatial uniformity across the network.

This methodology was demonstrated by up-scaling anorthite and kaolinite reaction rates under the acidic conditions relevant to geological CO<sub>2</sub> sequestration (Li et al 2006). Simulation results revealed that pore-scale concentrations of reactive species and reaction rates may vary spatially by orders of magnitude over millimeter length scales (see Figure 5). The resulting up-scaled reaction rates from the network model are significantly smaller than the continuum-scale reaction rates computed using uniform concentrations, demonstrating the importance of mass transfer limitations in porous media.

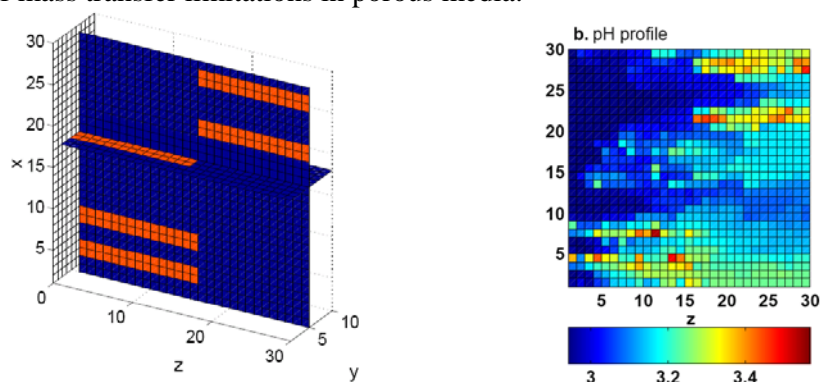


FIGURE 5. Left: An example of a network constructed for pore-scale network modeling. Pores are identified as being either reactive (red), or non-reactive (blue). Right: Steady state pH profile for the middle slice of the network after reaction with acidic brine entering from the left boundary. (Li et al. 2006).

The network modeling work was extended to examine the effects of variations in mineral spatial distributions on reaction rates and their scaling behaviors in porous media. Thirty-three

pore-scale network models were constructed to represent sandstones with anorthite and kaolinite present in various amounts and in different spatial patterns. With small percentages of reactive minerals, the scaling effects are large and the effect of spatial distribution is significant. Spatial distributions that enhance mass transport to and from reactive minerals, such as small mineral clusters or elongated clusters oriented transverse to flow, result in large anorthite dissolution rates and small kaolinite precipitation rates which are well represented by the continuum model. Conversely, scaling effects are largest when reactive minerals are closely clustered and oriented parallel to flow.

Additional work examined the applicability of volume-averaged concentrations, a mathematical analog of aqueous concentrations measured from groundwater samples, in determining mineral reaction rates in heterogeneous porous media (Li 2005). Network models were used to calculate volume-averaged concentrations and reaction rates calculated from these concentrations. Results showed that under many conditions the volume-averaged concentrations do not reflect reaction progress. Over the length scale of several millimeters, anorthite dissolution rates can be overestimated by a factor of four. For kaolinite, due to its highly nonlinear reaction rate law, even the reaction direction may be incorrectly determined, with precipitation predicted as dissolution. Conditions that homogenize the concentration fields, such as small reactive mineral clusters, abundant reactive minerals, or fast flow rates, increase mineral dissolution rates and minimize the errors introduced from volume-averaging. These results can have important implications for the interpretation of concentration data obtained from field investigation.

## 5. DISCUSSION AND CONCLUSIONS

Our network modeling work has illustrated the important role that physical and chemical heterogeneities play in up-scaling geochemical reaction rates to the scale of porous media. With regard to chemical heterogeneities, if “reactive” minerals are organized in clusters or in orientations that are parallel to flow then up-scaling is more nonlinear than otherwise. Given limited information about the nature and extent of this chemical heterogeneity, our modeling work to date has been based on hypothetical mineral spatial distributions.

The findings on mineral spatial patterns presented in this paper illustrate the valuable information contained in electron scanning maps that have compositional contrasting. Based on the sandstones studied here, “reactive” minerals, i.e. minerals other than quartz, are found in cements, grain inclusions and distinct grains. However, the reactive minerals that have the greatest amount of contact with pore space are largely authigenic, mature minerals that are not likely to play a large role in further weathering reactions. The less mature reactive minerals are found among the minerals in the “red” category. These are much less abundant and less likely to have contact with pore space. This has significant implications for reactive transport modeling which typically bases mineral reaction rates on bulk abundances. A more accurate measure would be the amount of pore space in contact with reactive minerals, and this appears to be a much smaller percentage than the total volume percentage. Shales and shaly sandstones have the largest abundance of reactive minerals, but reactive flow occurs in fractures rather than primary pore space. This presents a challenge to reactive transport modeling.

Sedimentary rock imaging is ongoing at Princeton and, in collaboration with Dr. Lindquist, we are generating an inventory of pore structures and reactive mineral spatial

patterns. Further development of network models will incorporate this information, in anticipation of understanding the reaction rate up-scaling and its relationship to these features.

## REFERENCES

- Bachu, S., W.D. Gunter, E.H. Perkins (1994) Aquifer disposal of CO<sub>2</sub>: Hydrodynamic and mineral trapping. *Energy Convers. Mgmt.* 35: 267-279.
- Bruant, R. G., Jr., M. A. Celia, A. J. Guswa, C. A. Peters (2002) Safe storage of CO<sub>2</sub> in deep saline aquifers. *Environ. Sci. Technol.* 36(11) :240A-245A.
- Christie, M.A., M.J. Blunt (2001) Tenth SPE comparative solution project: A comparison of upscaling techniques. *SPE Res. Eval. & Engin.* 4, 308-317.
- Bryant S.L., K.E. Thompson (2001) Theory, modeling and experiment in reactive transport in porous media. *Curr. Opin. Colloid Interface Sci.* 6, 217-222.
- Dagan, G. (1990) Transport in heterogeneous porous formations – spatial moments, ergodicity, and effective dispersion, *Water Resources Research*, 26 (6), 1281-1290.
- Espinoza, C., A. Valocchi (1997) Stochastic analysis of one-dimensional transport of kinetically adsorbing solutes in chemically heterogeneous aquifers, *Water Resour. Res.* 33, 2429-2445.
- Glimm, J, W.B. Lindquist, F. Pereira, Q. Zhang (1993) A theory of macrodispersion for the scale-up problem. *Trans. Porous Media* 13, 97-122.
- Jones, K.W., H. Feng, W.B. Lindquist, P.M. Adler, J.-F. Thovert, B. Vekemans, L. Vincze, I. Szaloki, R. Van Grieken, F. Adams, C. Riekkel (2003) Study of the microgeometry of porous materials using synchrotron computed microtomography. In: Applications of X-ray Computed Tomography in the Geosciences, F. Mees, et al. eds. Geological Society, London, Special Publications, 215, 39-49.
- Knauss, K., J. Johnson, C. Steefel (2005). Evaluation of the impact of CO<sub>2</sub>, cocontaminant gas, aqueous fluid and reservoir rock interactions on the geologic sequestration of CO<sub>2</sub>, *Chemical Geology*, 217, 339-350.
- Kreutzer-Walz, C. 2005. Stratigraphy and Petrography of Viking Sandstones in the Bayhurst Pool and Surrounding Areas, Southwest Saskatchewan. University of Regina, Dept. of Geology.
- Krinsley, D. H., K. Pye, S. Boggs Jr., N. K. Tovey (1998) Backscattered Scanning Electron Microscopy and Image Analysis of Sediments and Sedimentary Rocks. Cambridge University Press: New York, NY.
- Li, L. (2005) Scaling of Geochemical Reaction Rates Using Pore-Scale Network Modeling: An Investigation of Anorthite and Kaolinite Reaction Kinetics. Ph.D. Dissertation. Princeton University, Princeton, NJ.
- Li, L., C. A. Peters, M. A. Celia (2004) Upscaling calcite dissolution rates using network model simulations. *Water-Rock Interactions: Proc. Eleventh International Symposium on Water-Rock Interactions*, WRI-11. R. B. Wank and R. R. Seal II (Eds.), A. A. Balkema Publishers, London. pp 961-965.
- Li, L., C. A. Peters, M. A. Celia. (2006) Upscaling Geochemical Reaction Rates Using Pore-Scale Network Modeling. *Adv. Water Resour.*, In Press.
- Lichtner, P.C., C.I. Steefel, E. H. Oelkers (eds.) (1996) Reactive transport in porous media, *Rev. Mineral.* 34, Mineralogical Society of America.
- Neuman S.P., S. Orr. (1993) Prediction of steady-state flow in nonuniform geologic media by conditional moments - exact nonlocal formalism, effective conductivities, and weak approximation. *Water Resour. Res.* 29, 341-364.
- Reed, S. J. B. (1996) Electron Microprobe Analysis and Scanning Electron Microscopy in Geology. Cambridge: Cambridge University Press.
- Steefel, C.I., A.C. Lasaga. (1994) A coupled model for transport of multiple chemical species and kinetic precipitation/dissolution reactions with application to reactive flow in single phase hydrothermal systems. *Am. J. Sci.* 294, 529-592.
- Tompson, A.F.B. (1993) Numerical-simulation of chemical migration in physically and chemically heterogeneous porous-media, *Water Resour. Res.* 29, 3709-3726.
- Wallstrom, T.C., S.L. Hou, M.A. Christie, L.J. Durlofsky and D.H Sharp. (1999) Accurate scale up of two phase flow using renormalization and nonuniform coarsening. *Comput. Geosci.* 3, 69-87.
- White A.F., S.L. Brantley. (1995) Chemical weathering rates of silicate minerals: an overview. In: Chemical weathering rates of silicate minerals. *Rev. Mineral.* 31,1-22. Mineralogical Society of America.
- Xu, T., J. Apps, K. Pruess (2004). Numerical simulation of CO<sub>2</sub> disposal by mineral trapping in deep aquifers, *Applied Geochemistry*, 19 (6), 917-936.